Int. J. Electrochem. Sci., 8 **(2013)** 12531 - 12542

International Journal of
ELECTROCHEMICAL
SCIENCE
www.electrochemsci.org

Corrosion Behaviors of Q235 Steel in Indoor Soil

Ye Wan[1,2,3,*], *Lei Ding*[1], *Xiumei Wang*[1], *Yanbo Li*[1], *Hong Sun*[2], *Qing Wang*[1]

[1] School of Materials Science and Engineering, Shenyang Jianzhu University, Shenyang 110168, China
[2] School of Traffic and Mechanical Engineering, Shenyang Jianzhu University, Shenyang 110168, China
[3] State Key Laboratory for Corrosion and Protection, Institute of Metal Research, Chinese Academy of Sciences, Shenyang 110016, China
[*]E-mail: ywan@sjzu.edu.cn

Received: 13 August 2013 / *Accepted:* 29 September 2013 / *Published:* 20 October 2013

The corrosion behaviors of Q235 steel coupons were investigated via immersion and in-situ volumetric curve in soils with various moistures. The volumetric curves showed that the corrosion process of steel in the soils was a combination of activation and diffusion control. The cathodic part of the polarization curve obeyed Tafel law. Its extrapolation to the corrosion potentials gave the instantaneous corrosion rates much bigger than the average corrosion rate from mass loss. Nevertheless, both of the average and the instantaneous corrosion rates not only showed moisture had significant effect on soil corrosion of Q235 steel but the biggest was in 26% moisture soil being ca. 1.5× of the corrosion rate in the 12% moisture soil. The average corrosion rates for 7 days exposure were bigger than 21 days, owing to more corrosion products accumulating on the surface and hindering mass transfer at longer exposure than at initial immersion. Maximum pit depth grew fast and pit-covered length in per millimeter on the surface of the coupons (L_{pit}) slow during the first two exposure durations, and they were reversed during the third exposure duration.

Keywords: Q235 steel; Soil; Moisture content; Corrosion depth; Polarization

1. INTRODUCTION

Soil corrosion of steel is one of the main reasons for the reduced service life of underground pipelines [1-4]. The severity of soil corrosion depends on many environmental factors, such as temperature, moisture content, oxygen content, pH, and the soluble salts and was extensively studied and described [4-18]. While pit rate is of main interest many research has used measurement techniques such as mass loss and current flow but cannot define pit growth rates. This unfortunately reduces the utility of these studies [19]. Therefore, it is essential to find a useful method to identify the pit growth rates and pit process in soil.

Although the soil corrosion has a long and substantial history, and many research had focused on renewing those concepts and proposed some theoretical models [1,3,5], those studies have not led to the development of a comprehensive understanding or model of corrosion in soils [19]. In particular, it lacks clear measure methods to assess corrosion process of steel owing to the heterogeneous nature of soil.

Fortunately, the combination of average corrosion rate, surface profile, depth profile and corrosion current density provides a new approach to address this issue. Due to the large variability of environmental factors affecting soil corrosion, it is impractical to clarify the effects and corrosion processes of all factors in a multi-factor soil system.

It is known that the nature of soil corrosion of steel is an electrochemical process on the surface covered by liquid droplets or a thin liquid film if the moisture content is higher than a critical content. For this paper's purpose, one simple classified kind of soil based on one single environmental factor, moisture content, will be investigated via the archaeological methods. It should be interesting and possible to use those methods and refine the elucidation of pit growth rates and pit processes in soil. In addition, the effects of moisture content accompanied with exposure time on soil corrosion were identified via geomorphology and compared with different measure methods.

2. EXPERIMENT

2.1 Materials

Low carbon steel Q235 (0.14 C; 0.52 Mn; 1.42 Si; 0.015 P; 0.031 S [%.wt], balance Fe) with the size of 15 *mm* × 10 *mm* × 2.5 *mm* were cut in the purchased sheets and used during the experiments. The coupons were polished successively 400, 600, 800 and 1000 grits, degreased with alcohol and rinsed with deionized (DI) water, dried and kept in desiccators with silica gel for at least 24 hours. High purity DI water (Millipore > 20 MΩ cm) was used throughout.

The pH was 6.02 and the content of water was 24% for the underground soil in Shenyang, China. The soil type was loamy and its chemical composition was given in Table 1[20]. The soil was dried and sterilized at 105ºC in an oven for 5 hours. After the soil was cool, it was ground and screened with sieves of 2.35 *mm* to dispose of pebbles and roots. The soil was dried at 110ºC for 1 hour and cooled in air prior to being weighted. Consequently, DI water was added into the soils to prepare four kinds of indoor soils with 12% moisture, 19% moisture, 26% moisture and 33% moisture. The moisture content at 26% is close to the origin water content in Shenyang soil. It was observed for there was a thin water film on the whole surface of the 33% moisture soil, which demonstrated that the 33% moisture soil was a water saturation level. The soils were tightened and kept in soil chambers for 24 hours in advance. Q235 steel coupons were buried in the soils about 2 cm below the ground. The soil chambers were covered with a plastic film to keep the moisture from escaping throughout. Each chamber was at single moisture content. The buried tests were exposed in triplicate for every case. According to mass loss of every chamber's moisture, DI water was added into it immediately after

taking out the coupons to keep the constant moisture. The exposures were performed at room temperature. The temperature was measured from time to time and fluctuated between 18ºC and 21ºC.

Table 1. Chemical composition of the underground soil in Shenyang (mg/100g soil as received).

NO_3^-	Cl^-	HCO_3^-	Ca^{2+}	SO_4^{2-}
4.6	3.1	23.4	5.7	4.8
K^+	Na^+	Mg^{2+}	Organic carbon content	
0.2	1.4	3.2	2260	

2.2 Corrosion depth analysis

Over duration of 7 days, 14 days and 21 days, the average corrosion rate of Q235 steel was determined by mass loss. On completion of every exposure experiment, the coupons were removed from the soil chamber and performed mass loss. Three coupons, taken out from every chamber for the duration of the exposure, were performed mass loss according to the following procedure for the removal of corrosion products. The samples were first rinsed in deionized (DI) water for 2 minutes to remove soil and water-soluble corrosion products. Subsequently, the samples were treated in the following solution or proportionally more to remove the remainder of the corrosion products: 500 ml hydrochloric acid, 500 ml DI water and 20 g hexamethylenamine in every 1000 ml solution at the ambient temperature for 30 minutes. The majority of the experimental details have been discussed previously [21]. The mass loss during the rust removal was determined and corrected. The corrosion depth was calculated according to Eq.(1).

$$D = \Delta m/\rho \cdot S \qquad \text{Eq. (1)}$$

here, D is the corrosion depth of the sample; ρ is the density of the sample; S the surface area of the sample; Δm is the mass loss and equals to the difference between the origin mass and the derusted mass of the coupon.

2.3 Electrochemical analysis

The electrochemical experiments with low scan rate of 1 *mV/s* were conducted with an electrochemical instrument (LK3200A, Lanlike Co. Ltd., Tianjin, CN) combined with an electrochemistry software named LK3200A®. Voltammetry curves were performed to investigate the corrosion behavior of Q235 steel in soil. All the potentials were measured against an Hg/Hg_2Cl_2/saturated KCl reference electrode (SCE, + 0.2412 V/SHE). The potential range of voltammetry experiments was chosen between -1.2 V_{SCE} (V vs SCE) and -0.2 V_{SCE}. The solution used in electrochemical experiments was 3.5 (*wt*) % sodium chloride (NaCl) solution, with the pH set to 7.00 ± 0.05 with 0.1 $mol{\cdot}L^{-1}$ NaOH. NaCl solution was made from DI water and Sinopharm certified NaCl. A conventional three electrode cell was used for electrochemical studies. The cell exposed a

0.05 cm^2 portion of the coupons to be work electrodes. The counter electrode is a flat platinum mesh. All potentials were measured against the saturated calomel electrode (SCE) and quoted against this scale. Each electrochemical experiment was repeated at least three times on different occasions and the variation in response was less than 5 mV at room temperature.

2.4 Surface analysis

After the removal of corrosion products, the coupons' morphologies were observed using scanning electron microscopy (SEM) (S-4800, Hitachi, Japan). Imaging was performed with an accelerating voltage of 20.0 kV to produce high resolution images.

The derusted surfaces of the coupons, which have been buried in the 26% moisture soil for different time, were examined using a profilometer (Surtronic25, Taylor-Hobson, UK) to measure surface roughness as well as the width and the depth of pit.

3. RESULT AND DISCUSSION

3.1 Average corrosion rate

In completion of the exposure in different moisture soils, the coupons were dedusted and calculated the corrosion depth based on Eq.(1). In order to compare the corrosion rates obtained by mass loss with the corrosion rates calculated by corrosion current density (instantaneous corrosion rate, in the following sections), comparisons between the 7 days' data and the 21 days' results can be made by considering a common exposure time. For the current purposes, an exposure time of one year was used. Although we didn't know the corrosion kinetic of Q235 steel in the soils, we assumed the corrosion depths followed a linear kinetic. The corrosion depths for each version of the exposure (for instance different moisture and different exposure time) were scaled to one year based upon linear regression equations.

Fig.1 presents the annual average corrosion depth (average corrosion rate, hereinafter) and the standard error of Q235 steel after buried 7 days and 21 days in the soils with various moistures. The average corrosion rate decreased with exposure time. For instance, the average corrosion rate for 7 days was ca. 1.5× of 21 days at the 26% moisture soil. There was some relationship between average corrosion rate and moisture content, with average corrosion rate increasing up to 33% moisture content. It is clear that there was a great increase of average corrosion rate from 19% to 26 % moisture. In addition, the average corrosion rate didn't change much from the 26% to the 33% moisture soils for the two exposure durations. Interestingly, the standard errors at lower moisture were bigger than at higher moisture. In the case of 12% moisture, the standard errors were more than 35%. This is inherent attributed to soil's heterogeneous nature, which favored pit of the coupons. The lower the moisture content was, the more heterogeneous the soil was.

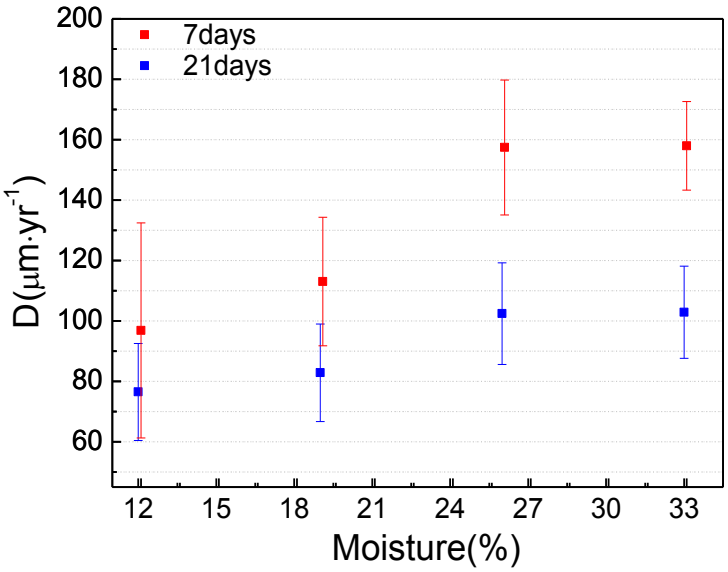

Figure 1. Average corrosion rate and standared error of the coupons buried in soils with various moisture contents for 7 days and 21 days.

3.2 Surface profile

In order to know the details of the coupons buried in different conditions, the surface images of the coupons were examined by SEM after removing the corrosion products. Fig.2 shows the images of the derusted surfaces of the coupons, which have been buried in the soils with 12% moisture and 19% moisture for 21 days respectively. It is clear that pit occurred for the coupons in the soils with 12% moisture and 19% moistures. Grinding strips were barely visible after exposed 21 days in the 19% moisture soil while slight in the 12% moisture soil. The coupon corroded severer and the corrosion area was bigger in the 19% moisture soil than in the 12% moisture soil. It can also be seen from Fig.2 that the boundary of pit became clear and developed outward its center and general corrosion began to appear when the moisture increased from 12% to 19%.

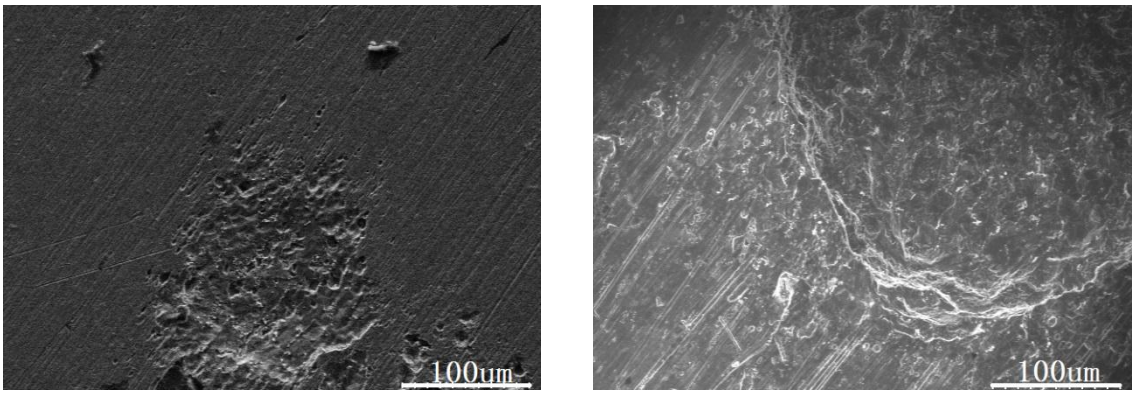

(a) (b)

Figure 2. Images of the derusted surface of the coupons, which have been buried in soil with (a) 12% moisture and (b) 19% moisture for 21 days.

Fig.3 presents the high- and low-magnification images of the coupons after buried in the soil with 26% moisture for different time. It is clear that the corrosion areas were increased with exposure time. It seemed the pit of the coupons was deeper if the coupons were exposed in the soils longer.

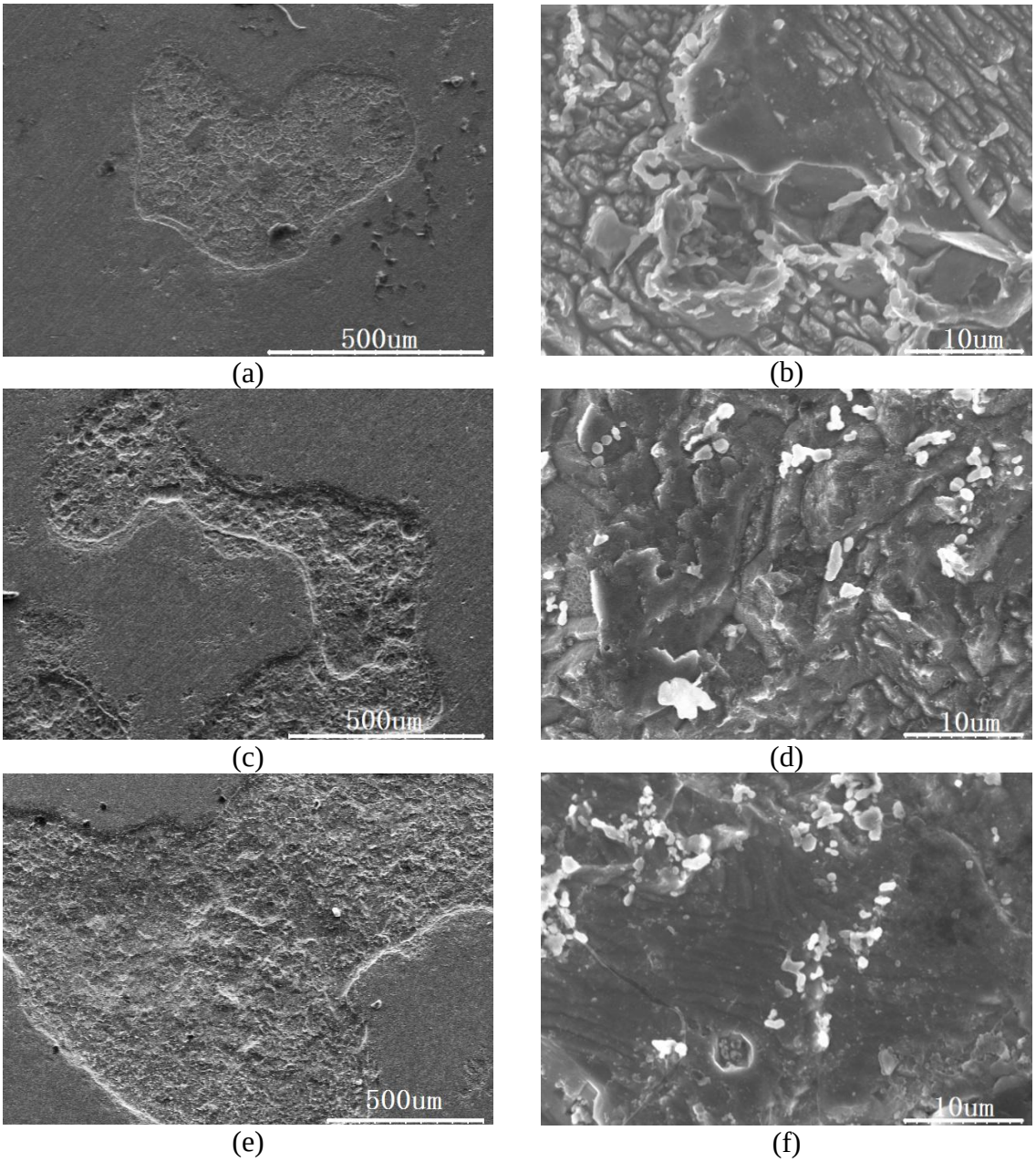

Figure 3. High- and low-magnification images of the derusted surfaces of the coupons, which have been buried in the 26% mositure soil for different time. (a) and (b) 7 days; (c) and (d) 14 days; (e) and (f) 21 days.

Comparing Fig.2 and Fig.3 (e), it is clear that the size of pit for the coupon in 26% moisture was far bigger than in the soils with 12% moisture and 19% moisture. No grinding strip could be seen for the coupon in 26% moisture soil. It can be deduced that the portion of general corrosion grew greatly with moisture content, and it was reversed for pit. This result was in agreement with Norin

[22] and Cole [19] that general corrosion was positively correlated with water content, these correlations were reversed for pit.

It was observed in the high-magnification images of the coupons that the dimples, formed by the removal of the crystal particles, were small in the pits of the coupon after exposed 7 days and derusted. The dimples in the pits of the coupons in the 26% moisture soil became bigger with increasing exposure time. Intergranular corrosion occurred in the coupon in the first exposure duration (7 days). Intercrystalline corrosion appeared and many cracks were formed in the third exposure duration (21 days).

3.3 Depth profile

Fig. 4 is the depth profiles of the derusted surfaces of the coupons, which have buried in the 26% moisture soil for different days. The surface roughness (R_a) of the derusted surfaces of the coupons, which have been buried in 26% moisture soil for different time, was calculated in the Surtronic25 profilometer. The results were shown in Table 2.

For the convenience, the width and the depth of the pits along per mm surface of the coupon were considered. The maximum pit depth for the coupon after 7 days was approximately 10 μm, and the maximum pit depths for the coupons after 14 days and 21 days were about 30 μm and 35 μm respectively. In order to compare the distribution of pit on the surface of the coupons, we defined L_{pit} as the pit-covered length in per millimeter on the surface of the coupons. Thereafter, L_{pit} can be deduced from Fig. 4 and listed in Table 2 as well. Table 2 illustrated that the pit depth didn't increase so much from 14 days to 21 days as that from 7 days to 14 days, but the areas covered by pit for the coupons exposed 21 days were larger than that exposed 14 days. It indicated that the maximum depth and the number of pit increased with exposure time.

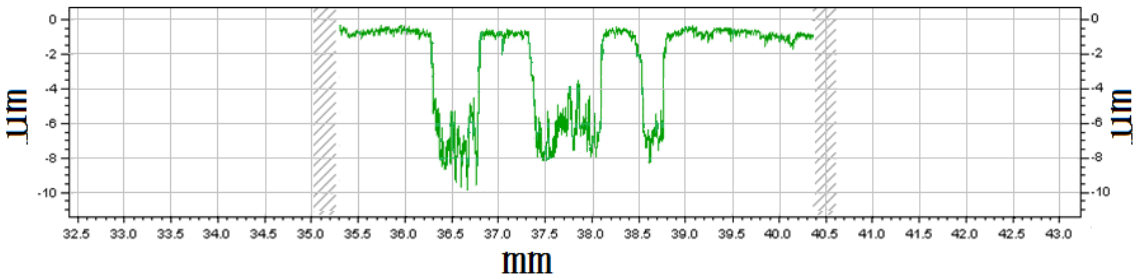

(a)

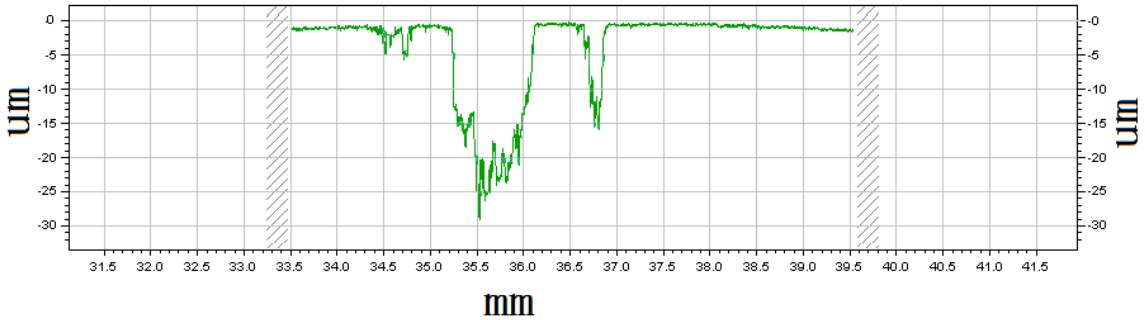

(b)

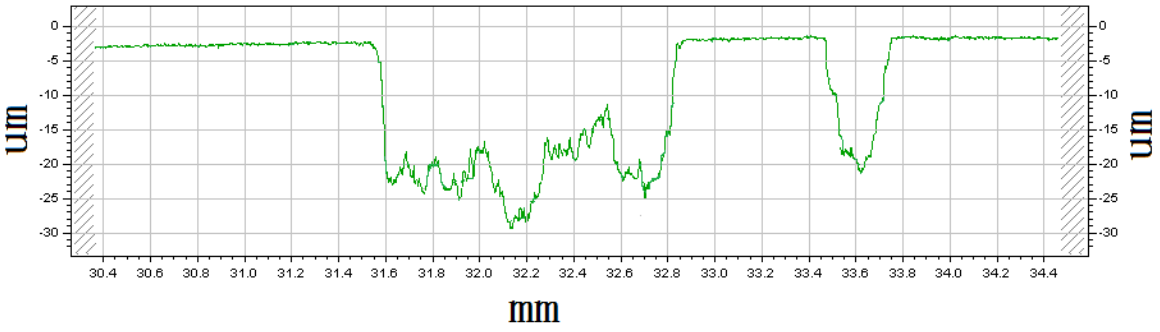

(c)

Figure 4. Depth profile of the derusted surfaces of the coupons, which have been buried different days in the 26% moisture soil for (a) 7 days, (b) 14 days, and (c) 21 days.

The results in Table 2 showed that the longer the coupons were exposed, the rougher their surfaces were and more pit covered the surfaces. The values of R_a illustrated that more areas of the coupons corroded for longer exposure, which was in agreement with the surface images. The results in Fig.4 and Table 2 show corrosion of the coupon developed transversely and longitudinally for longer exposure. Maximum pit depth grew fast and L_{pit} slow during the first two exposure durations, and they were reversed during the third exposure duration. In addition, there were more general corrosion and fewer pits at higher moisture content.

Table 2. ***R_a* and pit characteristic of the derusted surfaces of the coupons, which have been buried in the 26% moisture soil for different days.**

Exposure time (*day*)	7	14	21
Ra (μm)	0.5580	1.1248	1.4326
L_{pit} (mm)	0.273	0.275	0.347
Maximum pit depth (μm)	10	30	35

3.4 Volumetric curve

Fig.5 shows the volumetric curves of coupons in the soils with different moistures. The pHs of the four kinds of soils were measured shortly before running volumetric curve and were approximately 5.88, 5.92, 6.02 and 6.10 corresponding to the moisture contents of 12%, 19%, 26% and 33% respectively. According to Nernst equation, the H^+/H_2 equilibrium potential in the soils were equal to - 0.58812 V_{SCE}, - 0.59048 V_{SCE}, - 0.59638 V_{SCE} and - 0.6011 V_{SCE}, which indicated the main reaction in the cathodic polarization curve was oxygen reduction, seen in Re.(1).

$$O_2 + 2H_2O + 4e^- \rightarrow 4OH^- \qquad \text{Re. (1)}$$

It can be seen from Fig.5 that there was distinct linear domain between E and lg I in most of the cathodic curves, while no linear relationship appeared between E and lg I during anodic scan. The results meant reasonably that the kinetic of the cathodic reaction was controlled by mass transfer and

charge transfer. Therefore, the corrosion current had to be estimated via the extrapolation of cathodic Tafel lines [2]. According to this method, the cathodic Tafel lines was deducted and extrapolated up to corrosion potentials. These procedures were illustrated in Fig.5. The corrosion currents deduced from Fig.5 were for instance I_{corr} = 2.39 μA in the 12% moisture soil and I_{corr} = 4.04 μA in the 26% moisture soil. Corrosion current densities could be calculated according to the exposure work area (0.05 cm^2) in the soil.

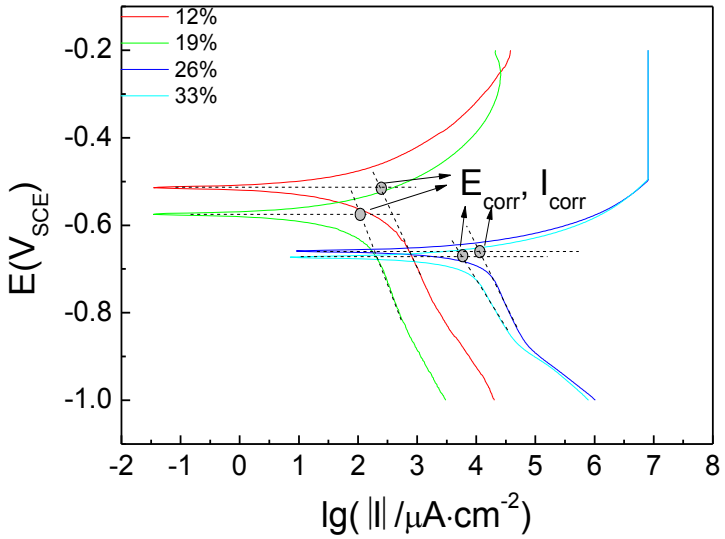

Figure 5. Volmmeograms of Q235 steel coupon in the soils with 12% moisture, 19% moisture, 26% moisture and 33% moisture respectively. Dash lines show the extrapolating method of the corrosion current.

According to Faraday's laws, the current density can be transformed to instantaneous corrosion rate as Eq. (2).

$$d = 3.28 \times 10^{-3} \frac{N}{n \cdot \rho} I_{corr} \qquad \text{Eq. (2)}$$

where, d is instantaneous corrosion rate ($mm{\cdot}year^{-1}$), N is molar mass ($g{\cdot}mol^{-1}$), n is chemical valence, I_{corr} is current density ($\mu A{\cdot}cm^{-2}$), and ρ is density ($g{\cdot}cm^{-3}$), of the metal respectively. F is Faraday' constant. $\rho = 7.8\ (g \cdot cm^{-3})$ for Q235 steel. The general anodic reaction for corrosion of Q235 steel in soil was Re. (2).

$$Fe - 2e^- \rightarrow Fe^{2+} \qquad \text{Re. (2)}$$

Thus, $x = 2$ and the instantaneous corrosion rates of the coupons in the four kinds of soils can be calculated according to Eq. (2).

Corrosion potentials and corrosion currents of the volumetric curves were estimated and summarized in Table 3. The instantaneous corrosion rates based on Eq. (2) were listed in Table 3 as well. The results in Table 3 indicated that instantaneous corrosion rates and the corrosion current and potential, derived from electrochemical experiments, were dependent on moisture content. The

corrosion processes were different for the four soils and could be divided into two groups. One is the soils with the lower moistures of 12% and 19%, and the other with the higher moistures of 26% and 33%. Corrosion potentials at the lower moistures were lower than at the higher moistures, and current densities were reversed. The instantaneous corrosion rates of the coupons in the 26% moisture and the 33% moisture soils were ca. 2× of the coupons in the 12% moisture and the 19% moisture soils. This indicated that higher moisture activated the anodic reaction and caused the corrosion rates in the higher moisture soils higher than in the lower moisture soils.

Table 3. **Electrochemical parameters and the instantaneous corrosion rates of Q235 steel coupon in the soils with different moisture content.**

Moisture content (%)	12	19	26	33
$E_{corr}(V_{SCE})$	- 0.514	- 0.575	- 0.659	- 0.673
$I_{corr}(10^{-6} A)$	2.39	2.07	4.04	3.77
$i_{corr}(\mu A \cdot cm^{-2})$	47.8	41.4	80.8	75.4
d (μm·year^{-1})	594.3	514.7	1004.6	937.5

The surface of the coupon in the 33% moisture soil was covered with a thin water film, which prevented oxygen transfer onto the surface of the coupon and hindered its corrosion for longer exposure. For the lower moisture content cases, such as 12% and 19% moisture, their instantaneous corrosion rates were almost the same. This result may be contributed to the charge transfer was the main rate-control step in the lower moisture soils during the initial exposure.

The corrosion rate, the corrosion current, and the surface images indicated that corrosion behaviors of the coupons barely changed from 26% moisture to 33% moisture. The possible reason is the mass transfer was the main rate-control step in the higher moisture soils during the initial exposure. It is known that chlorides in soil usually promote the corrosion of metal objects [23-24]. Although chloride content in the soils was decreased with moisture content, no significant correlation could be found between chloride content and corrosion probably because the concentration of chloride ion was low in this study. The electrochemical results revealed the soil corrosion of the coupon were transferring and activating control, which proved the corrosion theory of Nie et al. [25] and Cole [19] that the mass transfer of dissolved oxygen played an essential role in the kinetics of the corrosion process, and that the entire corrosion process was limited by a combination of activation and diffusion control.

It is not an easy way in a short exposure to establish an exact correlation between the corrosion rate and moisture because the corrosion process included pit accompanied with general corrosion. Nevertheless, we used a combination of series methods to study soil corrosion and got the developing trends of pit and general corrosion of Q235 steel in the soils. In particular, longer exposure of Q235 steel is underway.

4. CONCLUSIONS

Average corrosion rate and corrosion images of Q235 steel, buried in indoor loamy soils with various moisture contents and different time, were investigated via mass loss, morphology and in-situ electrochemical methods. Moisture content and exposure time were crucial factors controlling corrosion rate of Q235 steel in soil. Corrosion process of Q235 steel was a combination of charge transfer and mass transfer control. Maximum pit depth grew fast and L_{pit} slow during the first two exposure durations, and they were reversed during the third exposure duration. The maximum depth and the number of pit increased with exposure time. In addition, the portion of general corrosion grew greatly with moisture content, and it was reversed for pit. Intercrystalline corrosion occurred and many cracks were formed in the 26% moisture soil after buried 21 days.

The corrosion rate and the surface images of Q235 steel buried different durations (for instance 7 days, 14 days and 21 days) showed corrosion was severer in the 26% and 33% moisture soils than in the 12% and 19% moisture soils. The average corrosion rate at 26% moisture was approximately 157 $\mu m \cdot year^{-1}$, which was ca. 1.5× of 96.9 $\mu m \cdot year^{-1}$ at 12% moisture. The average corrosion rate of Q235 steel exposed 7 days was greater than 21 days. Actually, the surface of Q235 steel was covered with corrosion products during immersion exposure. The corrosion products hindered the mass transfer of dissolved oxygen and electrolyte consequently decreased the average corrosion rate.

The comparison between the instantaneous corrosion rates (no more than 20 minutes) and the average corrosion rates (up to 21 days) showed that the corrosion rates decrease with exposure time. Attributed to the formation and the accumulation of corrosion products on the surface of Q235 steel, the average corrosion rates were far smaller than the instantaneous corrosion rates but showed similar effects of moisture content on soil corrosion of Q235 steel as the instantaneous corrosion rate. Both of the corrosion rates in the 26% and the 33% moisture soils were much greater than that in the 12% and the 19% moisture soils.

ACKNOWLEDGMENTS

The authors gratefully appreciate the financial support from the National Natural Science Foundation of China (Grant No.: 51101106), the State Key Program of National Natural Science of China (Grant No. 51131007) and Program for Innovative Research Talent by the Ministry of Liaoning Education (Grant No.: LR2012019).

References

1. F. Caleyo, J.C. Velázquez, A. Valor and J.M. Hallen, *Corros. Sci*., 51(2009) 1925-1934
2. M. Barbalat, L. Lanarde, D. Caron, M. Meyer, J. Vittonato, F. Castillon, S. Fontaine and P. Refait, *Corros. Sci*., 55(2012) 246-253
3. A. Valor, F. Caleyo, J.M. Hallen and J.C. Velázquez, *Corros. Sci*., 66(2013): 78-87
4. M. Barbalat, D. Caron, L. Lanarde, M. Meyer, S. Fontaine, F. Castillon, J. Vittonato and P. Refait, *Corros. Sci.*, 73(2013) 222-229
5. J. Jiang, J. Wang, W.W. Wang and W. Zhang, *Electrochim. Acta*, 54(2009) 3623-3629
6. P. Corcoran, M.G. Jarvis, D. Mackney and K.W. Stevens, *J. Soil Sci*., 28(1977) 473-484
7. S.K. Gupta and B.K. Gupta, *Corros. Sci*., 19(1979) 171-178

8. T.J. Moore and C.T. Halmark, *Soil Sci. Soc. Am. J.*, 1987(51) 1250-1256
9. W.C. Robinson, Testing soil for corrosiveness, *Mater. Perform.*, 32(1993) 56-58
10. E. Levlin, *Corros. Sci*., 38(1996) 2083-2090
11. B. Spickelmire, *Mater. Perform*., 41(2002) 16-23
12. N.N. Aung and Y. Tan, *Corros. Sci*., 46(2004) 3057-3067
13. D. Neff, P. Dillmann, L. Bellot-Gurlet and G. Beranger, *Corros. Sci*., 47(2005) 515-535
14. C.A.M. Ferreira, J.A.C. Ponciano, D.S. Vatsman and D.V. Pérez, *Sci. Total Environ*., 388(2007) 250-255
15. Z.Y. Liu, X.G. Li, C.W. Du, G.L. Zhai and Y.F. Cheng, *Corros. Sci*., 50(2008) 2251-2257
16. M. Jeannin, D. Calonnec, R. Sabot and P. Refait, *Corros. Sci*., 52(2010) 2026-2034
17. V. Freitas C.H. Lins, M.L.M. Ferreira and P.A. Saliba, *J. Mater. Res. Technol*., 1(2012) 161-166
18. Y. Tan, *Corros. Sci*., 53(2011) 1145-1155
19. I.S. Cole and D. Marney, *Corros. Sci*., 56(2012) 5-16
20. X.M. Li, Z. Jin, W.Z. Liu, C. Sun, H.W. Zhang, J. Xu, M.C. Yan, C.K. Yu and Z.Y. Wang, *J. Chin. Soc. Corros. Protect.*, 33(2013) 216-220
21. Y. Wan, C.W. Yan and C.N. Cao, *J. Mater. Sci. Technol*., 19(2003) 453-455
22. M. Norin and T.G. Vinka, *Mater. Corros*., 54(2003) 641-651
23. G.H. Booth, A.W. Cooper, P.M. Cooper and D.S. Wakerley, *Brit. Corros. J*., 2(1967) 104-108
24. R.T. Foley, *Corros*., 26(1970) 58-70.
25. X.H. Nie, X.G. Li, C.W. Du and Y.F. Cheng, *J. Appl. Electrochem*., 39(2009) 277-282